Thermodynamic Studies on the Equilibrium Properties of a Series of Recombinant βW37 Hemoglobin Mutants†

Laurent Kiger,‡,§ Alexandra L. Klinger,‡ Laura D. Kwiatkowski,|| Alice De Young,|| Michael L. Doyle,‡ Jo M. Holt,‡ Robert W. Noble,|| and Gary K. Ackers*,‡

Department of Biochemistry and Molecular Biophysics, Washington University School of Medicine, St. Louis, Missouri 63110, and Department of Medicine, University at Buffalo Veterans Administration Medical Center, Buffalo, New York 14215

Received April 15, 1997; Revised Manuscript Received July 23, 1997

ABSTRACT: In human hemoglobin (Hb) the β37 tryptophan residue (βW37), located at the hinge region of the $\alpha^1\beta^2$ interface, forms many contacts with α subunit residues of the opposite dimer, in both the T and R quaternary structures. We have carried out equilibrium O_2 binding studies on a series of recombinant Hbs that have mutations at this residue site: βW37Y, βW37A, βW37G, and βW37E. Binding isotherms measured at high concentrations of these mutants were found to be shifted toward increased affinity and decreased cooperativity from that of the normal HbA_0 tetramer. Analysis of these binding isotherms indicated that amino acid substitutions at the β37 position could both destabilize the tetrameric form of the mutants relative to their constituent dimers and also alter cooperativity of the intact tetrameric species. These alterations from wild-type function are dependent on the particular side chain substituted, with the magnitude of change increasing as Trp is substituted by Tyr, Ala, Gly, and Glu. The dimer to tetramer assembly free energy of deoxy-βW37E, the most perturbed mutant in the series, was measured using analytical gel chromatography to be 9 kcal/tetramer less favorable than that of deoxy HbA_0. Stabilizing the βW37E tetramer by addition of IHP, or by cross-linking at the αK99 positions, does not restore normal O_2 binding behavior. Thermodynamic parameters of all the mutants were found to correlate with their CO binding rates and with their high-resolution X-ray crystal structures (see accompanying papers: Kwiatkowski et al. (1998) *Biochemistry 37,* 4325−4335; Peterson & Friedman (1998) *Biochemistry 37,* 4346−4357; Kavanaugh et al. (1998) *Biochemistry 37,* 4358−4373].

The abundance of naturally occurring hemoglobin mutants has resulted in many physical−chemical studies of mutational effects on cooperative oxygen binding. Such studies have been successful in identifying residues that are important for normal hemoglobin function, although the complete molecular mechanism of cooperativity has still not been delineated. Such insight most likely requires an understanding of mutational effects both in terms of altered local chemistry and also with consideration of the patterns of functional change with respect to the location of the mutation in the global molecular structure. The strategy of "mapping by structure−function perturbation" (Ackers & Smith, 1985, 1986; LiCata et al., 1993) has therefore been developed in this laboratory and has proven a powerful tool in a number of hemoglobin studies. In one such study (Turner et al., 1992), the overall cooperative free energies ΔG_C[1] for 60 naturally occurring mutant and chemically altered hemoglobins were analyzed showing the $\alpha^1\beta^2$ interface to be a unique structural location of the noncovalent bonding interactions that are energetically coupled to overall cooperativity. Two subsets of the 60 altered hemoglobins were characterized: one in which the magnitude of ΔG_C is solely dictated by structural location and another in which this response varies with side-chain type. Further investigation of residue position vs chemical nature is restricted in naturally occurring mutant hemoglobins, in part because only a limited number of substitutions at a particular amino acid location exist. In the present work we have pursued further the interplay between global and local mutational effects with equilibrium binding studies on a series of recombinant hemoglobins containing a range of substitutions at the β37 position (βW37Y, βW37A, βW37G, βW37E).[2]

† Supported by NIH Grants P01-HL084 and R37-GM24486 and NSF Grant DMB 9405492.

* To whom correspondence should be addressed at Department of Biochemistry and Molecular Biophysics, Washington University School of Medicine, 660 S. Euclid Ave., St. Louis, MO 63110. Telephone: (314) 362-0260. Fax: (314) 362-7183.

‡ Washington University School of Medicine.

§ Present address: INSERM U299, Hôpital de Bicêtre, F-94275 Le Kremlin-Bicêtre, France.

|| University at Buffalo VA Medical Center.

[1] Overall cooperative free energy (ΔG_C, i.e., the net cost of alterations in binding constants over all steps of oxygenation) is equal to the difference between binding free energies of cooperative tetramers and noncooperative dimers:

$$\Delta G_C \equiv \Delta G_4 - 2\Delta G_2$$

where ΔG_4 is the overall free energy for tetramer binding and ΔG_2 is that over the two steps of dimer binding. ΔG_C measures the energetic cost of modulating the binding free energy in the tetramer from its value in the constituent α and β subunits (or noncooperative $\alpha\beta$ dimers). The path independence of free energy (Scheme 1) leads to an equivalent expression for ΔG_C as

$$\Delta G_C = {}^4\Delta G_2 - {}^0\Delta G_2$$

where ${}^4\Delta G_2$ and ${}^0\Delta G_2$ are the deoxy and oxy dimer to tetramer assembly free energies, respectively.

S0006-2960(97)00868-4 CCC: $15.00
Published on Web 03/17/1998

The β37 residue of human hemoglobin (HbA_0)[3] is located in the C helix corner "hinge region" of the $\alpha^1\beta^2$ interface involving several important contacts between the two dimers, both in the unligated and ligated tetrameric structures (Dickerson & Geis, 1983; Perutz, 1970). In normal HbA_0, β37 tryptophan interacts with arginine (αR92), aspartate (αD94), and proline (αP95) residues of the α FG corner and also with a tyrosine (αY140) from the N-terminal peptide (Baldwin & Chothia, 1979). Properties of the naturally occurring β37 mutants Rothschild (βW37R) (Sharma et al., 1980; Turner et al., 1992), Hirose (βW37S) (Sasaki et al., 1978, Turner et al., 1992), and Howick (βW37G) (Brittain, 1994; Owen et al., 1993), as well as the recombinant Hbs βW37T (Vallone et al., 1996) and βW37F (Ishimori et al., 1992), showed that replacement of Trp results in significantly increased tetramer dissociation in both the deoxygenated and oxygenated states. For example, the Hb Hirose tetramer is 1500 times less stable than HbA_0 in the deoxy state and 100 times less stable in the oxy state (Turner et al., 1992). At the micromolar protein concentrations used in most of the previously published binding studies the low populations of tetrameric molecules in samples of these destabilized β37 mutants have prevented accurate evaluation of tetramer binding energetics. In addition, when high concentrations of Hb were studied, the very low O_2 partial pressures at which these high-affinity mutants bind were below the accuracy range of the electrode methods employed. Thus, the apparent reduced cooperativity and increased affinity observed in O_2 binding have usually been attributed solely to an increased population of dimers.

In this study, however, O_2 binding isotherms have been measured for the β37 mutant series at high total protein concentration using the dilution method for deoxygenation employed by the Gill cell (Dolman & Gill, 1978). In agreement with previous work, the binding curves of this series are all found to be shifted, relative to normal HbA_0, toward higher affinity and lower cooperativity. Analysis of these accurate O_2 binding isotherms, in combination with estimates of the deoxy assembly free energies for these mutants, made it possible to extract information pertaining to the binding affinities of the pure mutant tetramers. The effects of mutation on the oxygen binding reactions could then be resolved separately from the dimer to tetramer assembly reactions. Our results show that enhanced tetramer dissociation alone is insufficient to describe the shifts in oxygen binding curves of the mutants from that of normal Hb, and that the pure mutant tetramers are perturbed. The extent of destabilization, coupled with the perturbation in tetramer binding, follows an order, βW37Y < βW37A < βW37G < βW37E, that corresponds with X-ray structural findings and with kinetic results on the same mutants series (Kavanaugh et al., 1998; Kwiatkowski et al., 1998). Further investigations on the highly perturbed dimer−dimer interface were carried out by stabilizing the tetrameric form of the most perturbed mutant (βW37E) with IHP. Additionally, the O_2 binding properties were determined for the βW37E mutant when constrained into the tetrameric form by fumaryl cross-linking at the αK99 positions. While both the allosteric effector and the cross-linker were effective in increasing the population of tetramers, neither had significant effect on the mutant O_2 binding isotherms.

EXPERIMENTAL PROCEDURES

Materials. Hemoglobin A_0 (HbA) was prepared by the method of Williams and Tsay (1973) from hemolysates of freshly drawn blood. β37 mutant globins were expressed in *Escherichia coli*, purified, refolded with the heme prosthetic group, and assembled with natural human α chains as described in detail in the accompanying paper (Kwiatkowski et al., 1998). The β37 mutant hemoglobins contain an additional β1 Val → Met mutation since the normal terminal Met is not cleaved by the processing enzyme in *E. coli* (Hernan et al., 1992). HbA_0 cross-linked between α^1-Lys99 and α^2Lys99 by reaction with bis(3,5-dibromosalicyl) fumarate (Chatterjee et al., 1986) was highly purified as described in Kwiatkowski et al. (1998). Cross-linked β37 mutants were prepared by regeneration of the β globins with purified cross-linked α chains.

Measurements of O_2 Binding Equilibria. (A) Gill Cell Measurements. Binding isotherms of the mutants were measured with a membrane-covered, thin-layer optical cell (Dolman & Gill, 1978). Approximately 10 μL of a 500 μM−1 mM [heme] sample in standard buffer (0.1 M Tris-HCl, pH 7.4 at 21.5 °C, 0.1 mM NaCl, 1 mM Na_2EDTA) was loaded onto the cell. To minimize perturbation of the standard buffer pH, enzyme concentrations of the reductase system enzymes (Hayashi et al., 1973) were diluted 10-fold from those described previously (Mills et al., 1976). Oxy and deoxy spectra were recorded before and after the deoxygenation process, showing less than 1% *met*-hemoglobin formation.

Samples were equilibrated with humidified air and deoxygenated with dilutions of humidified pure nitrogen gas. The dilution factor at each step was 0.5945 ± 0.0015. The change in fractional saturation after each dilution step was recorded at 415 nm with a Cary 3 spectrophotometer (Varian Instruments, Inc.). Atmospheric pressure was measured before each experiment with a Nova barometer (Princo Instrument, Inc.). Temperature was maintained at 21.5 °C with an RTE-110 thermostated bath (Neslab). O_2 molarities were calculated using the Henry law constant 1.78×10^{-6} M $Torr^{-1}$ (Wilhelm et al., 1977).

Initial characterization of oxygen binding properties for the mutants was provided by the partial pressures at half-

[2] Because the terminal methionine residue of the expressed β globins is not cleaved by the *E. coli* enzyme processing system, it is of interest that the resultant recombinant mutants at the β N-terminal position (βV1M, βV1A, and β1 + Met) have been found to have global functional properties similar to those of normal HbA_0 (Doyle et al., 1992a). In this study the recombinant Hbs all contain the βV1M substitution in addition to any other mutation.

[3] Abbreviations: bis-Tris, [bis(2-hydroxyethyl)aminotris(hydroxymethyl)methane; Tris, tris(hydroxymethyl)aminomethane; HbA_0, human hemoglobin major component; IHP, inositol hexaphosphate; metHb, hemoglobin with iron oxidized to Fe(III); CNmetHb, hemoglobin with iron oxidized to Fe(III) and bound to CN; Na_2EDTA, disodium ethylenediaminetetraacetate.

[4] The single isotherm data sets could provide only enough information with which to determine the overall binding free energy (ΔG_2) for each of the mutant dimers. We assume noncooperative binding in which the α and β subunits have the same affinity, giving $\Delta G'_{21} = \Delta G'_{22} = (1/2)\Delta G_2$. For all the mutant dimers, then, the intrinsic stepwise binding free energy for binding 1 mol of O_2 is −7.9 ± 0.1 kcal/mol.

saturation (P_{50}) and the median partial pressures (P_{med}) calculated with the relation:

$$\log(P_{med}) = \sum \log(X_i X_{i-1})^{1/2} \Delta A_i / \sum \Delta A_i \quad (1)$$

where ΔA_i is the change of absorbance after the ith dilution step from the O_2 partial pressure X_{i-1} to X_i (DiCera & Gill, 1988).

Data transformed into fractional saturation ($\bar{Y}$), were analyzed using nonlinear regression according to eqs 2−4, which portray on model-independent grounds the ligand-linked equilibrium between dimers and tetramers as a function of the four tetramer Adair constants (K_{41}, K_{42}, K_{43}, K_{44}), the two dimer Adair constants (K_{21}, K_{22}), the deoxy dimer to tetramer equilibrium constant ${}^0K_2$, and the total protein concentration P_t (Ackers & Halvorson, 1974) such that

$$\bar{Y} = \frac{Z'_2[D] + Z'_4 {}^0K_2[D]^2}{2Z_2[D] + 4Z_4 {}^0K_2[D]^2} \quad (2)$$

where

$$Z_2 = 1 + K_{21}[X] + K_{22}[X]^2$$

$$Z'_2 = K_{21}[X] + 2K_{22}[X]^2$$

$$Z_4 = 1 + K_{41}[X] + K_{42}[X]^2 + K_{43}[X]^3 + K_{44}[X]^4 \quad (3)$$

$$Z'_4 = K_{41}[X] + 2K_{42}[X]^2 + 3K_{43}[X]^3 + 4K_{44}[X]^4$$

and

$$[D] = \frac{-Z_2 + \sqrt{Z_2^2 + 4Z_4 {}^0K_2 P_t}}{4Z_4 {}^0K_2} \quad (4)$$

${}^0K_2$ values were constrained in the fitting process to values determined independently from analytical gel chromatography (AGC) experiments described below or from the ratio of fast and slow CO binding amplitudes described in the accompanying kinetics paper (Kwiatkowski et al., 1998).

Hill coefficients for the *mixture* of dimers and tetramers were calculated by transforming the fractional saturation, $\bar{Y}$, as follows:

$$n_H = \frac{d[\ln(\bar{Y}/(1-\bar{Y}))]}{d \ln X} \quad (5)$$

All data were analyzed by the nonlinear least-squares program NONLIN (Johnson & Frasier, 1985) on a Hewlett-Packard 9000/710 workstation.

(B) Imai Cell. Oxygen binding isotherms of cross-linked HbA_0 and cross-linked Hb βW37E were measured using the spectrophotometric apparatus based on the design of Imai (1981). Hemoglobin solutions (10 μM heme in standard buffer with and without 100 μM IHP) were stirred in a sample cell (2.3 cm path length) and equilibrated with humidified O_2. Samples were then continuously deoxygenated by slowly flowing humidified N_2 gas over the surface of the solution. Spectra were measured every 1 nm between 800 and 400 nm at approximately 30 s time intervals during the deoxygenation process using a Cary 4 spectrophotometer scan rate of 900 nm/min. Dissolved O_2 concentration was monitored with a YSI 5331 oxygen probe (Yellow Springs Instrument Co., Yellow Springs, OH). Output from the probe was amplified with a Keithley 150B microvolt ammeter and then digitized with an HP 3478A multimeter. The digitized signal was transferred via a GPIB port to a Pentium computer (Dell) that also controls the spectrophotometer under the OS/2 operating system. Each oxygen electrode reading was correlated to the spectrum being measured using a data acquisition program written with Borland C++ for OS/2.

The oxygen electrode millivolt reading has linear response to the oxygen pressure as verified with certified gas mixtures of O_2 in N_2 (Linde Gases). The millivolt readings were converted to O_2 partial pressures using the relation:

$$P = \frac{(P_{atm} - P_{vap})(m\upsilon - m\upsilon_0)}{(m\upsilon_{atm} - m\upsilon_0)} \quad (6)$$

where P is the partial pressure of oxygen, P_{atm} is the barometric pressure, P_{vap} is the sample vapor pressure (19 mmHg), $m\upsilon_0$ is the millivolt reading under pure nitrogen, and $m\upsilon_{atm}$ is the reading under pure O_2. O_2 partial pressures were converted to molarities using the Henry law constant 1.78×10^{-6} M Torr^{-1} (Wilhelm et al., 1977).

Isotherms were constructed from the multiwavelength data by normalizing the change in absorbance at 415 nm. Binding isotherms of the cross-linked molecules were analyzed to obtain the four tetramer Adair constants by fitting to the equation:

$$\bar{Y} = \frac{K_{41}X + 2K_{42}X^2 + 3K_{43}X^3 + 4K_{44}X^4}{4[1 + K_{41}X + K_{42}X^2 + K_{43}X^3 + K_{44}X^4]} \quad (7)$$

where K_{4l}, K_{42}, K_{43}, and K_{44} are the classical Adair constants which account for the four stoichiometric levels of binding. For the cross-linked mutant βW37E, oxygen binding experiments were repeated at high concentrations in the Gill cell due to inaccuracy of the oxygen electrode at very low partial pressures (Doyle & Ackers, 1992).

Data were manipulated using the matrix handling program MATLAB (The Mathworks, Inc., Natick, MA). Regression analysis was performed with the nonlinear least-squares fitting program NONLIN (Johnson & Frasier, 1985). Both MATLAB and NONLIN were run on a Hewlett-Packard 9000/710 workstation.

Analytical Gel Chromatography. Dimer−tetramer assembly free energies of selected deoxygenated mutants were determined by large zone analytical gel chromatography in the presence and absence of 500 μM IHP using a column with a thermostated jacket (Valdes & Ackers, 1979). The column temperature was maintained at 21.5 °C with a Lauda K2/R thermoregulator (Brinkmann Instruments). Elution profiles were recorded in a flow-cell cuvette using a Shimadzu UV-150-02 spectrophotometer. Anaerobicity was maintained with a Coy Laboratory Products Type B anaerobic chamber equipped with three catalyst boxes in a N_2/H_2 gas mixture. Oxygen partial pressure inside the chamber was monitored continually with a Coy Model 10 gas analyzer and was observed never to exceed the 1 ppm detection limit of the analyzer. Since the median oxygen affinity for the

βW37E mutant is less than 1 Torr, a trace amount of sodium dithionite (Hoechst Celanese, Portsmouth, VA) was added to the samples. The flow was driven with either a Dynamax/Rainin Model RP-1 or an LKB 10200 Perpex peristaltic pump and was found during a 24 h period to have a constant rate to within $\pm$0.02 mL/h.

For a dimer to tetramer associating macromolecule, the centroid elution volume (V_e) corresponding to a given Hb plateau concentration (P_t) depends on the fractions of dimers and tetramers, f_D and f_T, and their respective elution volumes, V_D and V_T, according to the relation:

$$V_e = V_D f_D + V_T f_T \quad (8)$$

where f_D is given by

$$f_D = \frac{-1 + \sqrt{1 + 4K_2P_t}}{2K_2P_t} \quad (9)$$

In eq 9, P_t is total heme concentration and K_2 is the dimer to tetramer equilibrium constant. Measured elution volumes as a function of total protein concentration were fit using eqs 8 and 9 with either the nonlinear least-squares fitting program NONLIN (Johnson & Frasier, 1985) or the experimental data fitting package, Scientist (MicroMath Scientific Software, Salt Lake City, UT). The data and the nonlinear least-squares fits were plotted in terms of the weight-average partition coefficient $\bar{\sigma}_w$:

$$\bar{\sigma}_w = \frac{V_e - V_0}{V_i} \quad (10)$$

where V_0 and V_i are the void and internal volumes determined from small-zone experiments on the nonassociating molecules glycylglycine and blue dextran.

RESULTS

Gill Cell Oxygen Binding Experiments. Since mutations at the β37 position are known to destabilize the tetrameric form of the molecule, increasing the population of high-affinity dimers, their O_2 binding isotherms were measured with the thin-layer technique of Gill (Dolman & Gill, 1978). This method uses high sample concentrations, shifting the assembly equilibrium toward tetramer. In addition, the dilution protocol with which the Gill cell is deoxygenated allows for detailed shape analysis of isotherms at very low O_2 concentrations (Doyle & Ackers, 1992).

Binding isotherms for four βW37 mutants (βW37Y, βW37A, βW37G, βW37E) are shown in Figure 1. The smooth lines through the data are least-squares fits (under assumptions described below) of eqs 2−4, i.e., the binding isotherm formulation for an equilibrating mixture of dimers and tetramers, to the data. Corresponding Hill transformations for each mixture of dimers and tetramers are given as an inset. Shown for comparison are isotherms simulated using the resolved O_2 binding constants for the dimeric and tetrameric species of HbA_0 (Chu et al., 1984).

The mutant isotherms exhibit, to differing extents, an increase in O_2 binding affinity and a decrease in cooperativity relative to the HbA_0 tetramer as judged by inspection of Figure 1. The four mutants can also be ordered with respect to the extent of mutational perturbation on oxygen binding

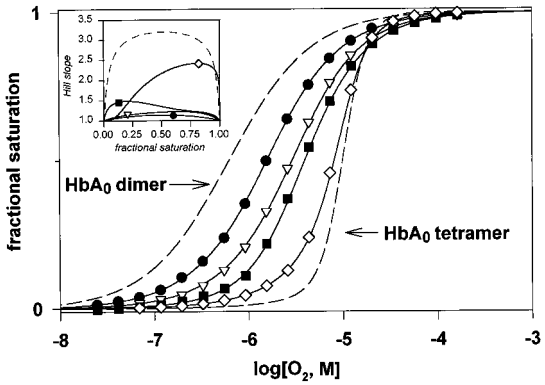

FIGURE 1: O_2 binding isotherms of β37 Hb mutants. Symbols are the fractional change in absorbance at 415 nm as measured with the Gill cell for (◇) 420 μM [heme] βW37Y, (■) 635 μM [heme] βW37A, (▽) 675 μM [heme] βW37G, and (●) 765 μM [heme] βW37E. Solid lines are best nonlinear regression fits of eqs 2−4 to the data. Dashed lines are simulated isotherms for pure HbA_0 dimers or tetramers as indicated. Solution conditions were 0.1 M Tris, 0.1 M NaCl (0.18 M total chloride), and 1 M Na_2EDTA, pH 7.4 at 21.5 °C. (Inset) Hill transformations of O_2 binding isotherms for HbA_0 tetramers (dashed line) and the mutants.

Table 1: General O_2 Binding Parameters of βW37 Mutants[a]

	βW37E[b]	βW37G[b]	βW37A[b]	βW37Y[b]	HbA_0
P_{50} (Torr)	0.9	1.6	2.2	4.4	5.5
P_{med} (Torr)	0.9	1.5	2.2	3.8	5.4
n_H	1.1	1.2	1.4	2.4	3.2

[a] Binding curves were measured under standard conditions (0.1 M Tris, 0.1 M NaCl, and 1.0 mM Na_2EDTA, pH 7.4 at 21.5 °C) in the presence of the enzyme reductase system of Hayashi et al. (1973).[b] Also contain the βV1M mutation (see footnote 2).

properties, so that βW37Y < βW37A < βW37G < βW37E. This order is apparent in Figure 1 and can be further assessed from the partial pressures at half-saturation (P_{50}), the median partial pressures (P_{med}), and the maximum Hill coefficients (n_H) given in Table 1.

Analytical Gel Chromatography (AGC) of the βW37E Mutant. Weight-average partition coefficients $\bar{\sigma}_w$ for deoxy-βW37E as a function of log(P_t), obtained from AGC experiments, are shown in Figure 2. Measurements at high P_t could not be conducted due to scarcity of the recombinant protein. The best least-squares fit of a dimer to tetramer assembly curve to the available deoxy data is shown. This fit gave an assembly free energy ($^0\Delta G_2$) of −4.22 kcal/mol for the deoxy mutant tetramer. βW37E is thus greatly destabilized with respect to normal deoxy-HbA_0 ($^0\Delta G_2$ = −14.4 kcal/mol). Shown for comparison in Figure 2 are the $\bar{\sigma}_w$ vs log(P_t) data points for *oxy*-HbA_0 and the best least-squares fit to these values ($^0\Delta G_2$ = −8.15 kcal/mol).

Analysis To Resolve βW37E Dimer and Tetramer Binding Parameters. To rigorously analyze the βW37E mutant O_2 binding behavior, the energetic parameters must be resolved from eqs 2−4 describing fractional saturation of an equilibrium mixture of dimers and tetramers at a given protein concentration. These equations contain seven parameters comprising the stoichiometric binding constants of dimers and tetramers (K_{21}, K_{22}, K_{41}, K_{42}, K_{43}, and K_{44}) and the equilibrium constant ($^0K_2$) for deoxy dimer to tetramer assembly. To uniquely determine each of these parameters for highly cooperative HbA_0, it is necessary to simultaneously fit a series of O_2 binding curves at varying protein concentra-

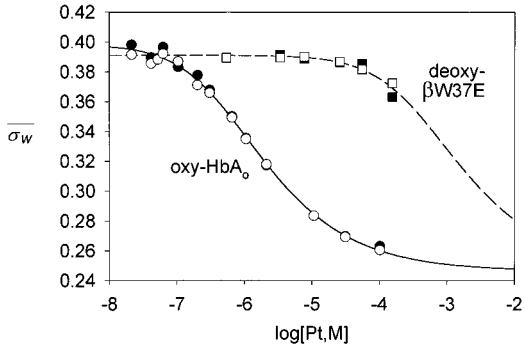

FIGURE 2: Subunit assembly of βW37E by AGC. Weight-average partition coefficients vs logarithm of total [heme] for normal oxy-Hb (circles) and deoxy βW37E (squares). Pairs of data points at each Hb concentration correspond to values determined from the leading (filled symbols) and trailing (open symbols) boundaries of each large-zone experiment. Solid curves are dimer to tetramer assembly isotherms simulated using the best fit free energies of −8.15 kcal/mol (oxy-HbA_0) and −4.22 kcal/mol (deoxy-βW37E). Experimental conditions were 0.1 M Tris, 0.1 mM NaCl (0.18 mM total chloride), and 1 mM Na_2EDTA, pH 7.4 at 21.5 °C.

tions and to constrain $^0K_2$ and $^4K_2$ to values determined by independent measurements (Johnson et al., 1976). Due to the decreased cooperativity of the βW37E mutant, however, the population of partially oxygenated tetramers is not as highly suppressed. The binding parameters may therefore be resolved by nonlinear least-squares fitting of eqs 2−4 to a single binding isotherm if an initial constraint is placed on $^0K_2$ to a value determined by independent measurement.

The first column of Table 2 gives the results of this analysis. The overall dimer binding (ΔG_2) is reduced from −16.7 ± 0.1 kcal/mol for HbA_0 to −15.7 ± 0.1 kcal/mol for βW37E. To further minimize the variance to the data, $^0\Delta G_2$ was allowed to vary from the value estimated from the AGC experiments after convergence on the dimer and tetramer fitting parameters was reached. The best fit gives $^0\Delta G_2$ equal to −5.2 ± 1.0 kcal/mol. While this value differs from that estimated using AGC, the two numbers must be considered indistinguishable within error considering the paucity of AGC data points within the concentration range where dimer to tetramer assembly transition occurs (Figure 2). At the high Hb concentration binding isotherm measurement (765 mM [heme]), the fraction of hemes in tetrameric form was approximately 65%. Thus the stepwise binding free energies could be resolved for the βW37E tetramer form (i.e., $\Delta G'_{41}$, $\langle\Delta G'_{42,43}\rangle$, $\Delta G'_{44}$). The tetramer binding free energies showed no cooperativity, and each intrinsic stepwise binding free energy was identical with that of the dimer ($\Delta G'_{21} = \Delta G'_{22} = 1/2\Delta G_2$).

Analysis To Resolve βW37G, βW37A, and βW37Y Dimer and Tetramer Binding Parameters. The measured binding isotherms for the remaining three mutants, βW37G, βW37A, and βW37Y, were similarly fit with the linkage eqs 2−4 so as to resolve their separate dimer and tetramer binding parameters. $^0\Delta G_2$ values were not determined using the AGC technique but rather were constrained to values estimated from the ratio of amplitudes observed for the slow (tetramer) and fast (dimer) rates of CO binding (see Table 2 of Kwiatkowski et al. (1998)). In the case of βW37G these amplitudes are not well resolved, since the two rates differed by no more than a factor of 2.5. Amplitudes of the two rates were therefore arbitrarily constrained to be equal, yielding a value for $^0\Delta G_2$ of −8.1 kcal/mol. Recently, however, the deoxy assembly free energy of a naturally occurring βW37G mutant (Hb Howick) has been determined under slightly different conditions (0.05 M Tris, pH 7.5, 0.1 M NaCl, 1 mM Na_2EDTA at 25 °C) to be −7.5 kcal/mol (Brittain, 1994). Correcting this value for the temperature difference between the respective conditions by using an enthalpy value of 30 kcal/mol for the deoxy assembly reaction (Huang & Ackers, 1995; Mills et al., 1979), a $^0\Delta G_2$ value of −7.7 kcal/mol is calculated for Hb Howick at 21.5 °C. This value can be compared with the −8.1 kcal/mol value that would result for $^0\Delta G_2$ if 50% of the hemes were in dimeric form at 2 mM [heme]. Use of either value as a constraint leads to essentially identical values for the recombinant βW37G dimer and tetramer binding free energies.

Results of the fitting analyses for all the mutants are given in Table 2. The same pattern resulting from the particular amino acid substitution on P_{50}, P_{med}, and n_H is also seen on the mutant $^0\Delta G_2$ values which range from −5.2 kcal/mol for βW37E to −9.1 kcal/mol for βW37Y. The deoxy mutant tetramer destabilization from normal HbA_0 is paralleled by more negative initial stepwise O_2 binding free energy values ($\Delta G'_{41}$) of the mutants from that of HbA_0. That is, as deoxy tetramer stability decreases, affinity at the first binding step increases.

Effect of IHP on Deoxy Subunit Association of βW37E and βW37G. Subunit assembly of deoxy-βW37E and deoxy-βW37G mutants in the presence of 500 μM IHP was measured by analytical gel chromatography (AGC). The results are depicted in Figure 3 as $\bar{\sigma}_w$ vs log(P_t). Also shown is a standard curve for cyanomet-HbA_0. Smooth curves show the dimer to tetramer transition, simulated using the deoxy assembly free energy ($^0\Delta G_2$) that was resolved from the least-squares fit to these data. IHP is known to stabilize the deoxy form of HbA_0 (Robert et al., 1988; White, 1976). We have measured this stabilization under our standard conditions using the haptoglobin kinetics technique (Ip et al., 1976; data not shown) to be ∼2 kcal/mol. It was seen that IHP has a similar effect on $^0\Delta G_2$ for the mutants βW37E and βW37G—increasing their tetramer stability from −5.2 to −7.3 kcal/mol and from −8.1 to −9.8 kcal/mol, respectively. The $^0\Delta G_2$ values for unmodified βW37E and HbA_0 in the presence and absence of IHP are listed in Table 3.

Effects of IHP on O_2 Binding of Unmodified HbA$_0$ and βW37E. Figure 4 includes (a) the simulated isotherm for tetrameric HbA_0 (thick dot-dashed line), (b) the measured isotherms for HbA_0 in the presence of IHP (filled circles without cross-hairs), and (c) the βW37E isotherms in the presence and absence of IHP (filled and empty triangles without cross-hairs, respectively). Results from nonlinear least-squares fits of the linked dimer and tetramer binding equations to these isotherms are depicted by thin solid lines and are listed in Table 3. In order for the effect of IHP on the tetrameric form of the molecules to be observed, experiments were conducted in the Gill cell at high P_t with ∼2 mol of IHP/tetramer. Under these conditions the effect of IHP on HbA_0 was found to be an approximately 3 kcal/mol decrease in overall oxygen binding affinity (ΔG_4) and a slight decrease in its overall cooperativity. The effect of IHP on $^0\Delta G_2$ for HbA_0 cannot be deduced from the O_2

Table 2: Thermodynamic Parameters Characterizing Recombinant Mutant and Wild-Type Hbs Determined by Analysis of O_2 Binding Curves[a]

	βW37E[e]	βW37G[e]	βW37A[e]	βW37Y[e]	HbA_0
			Overall Binding Free Energies		
ΔG_2	−15.7 ± 0.1	−15.8 ± 0.2	−15.8 ± 0.2	−15.6 ± 0.2	−16.7 ± 0.1
ΔG_4	−31.3 ± 0.1	−29.8 ± 0.1	−28.7 ± 0.2	−27.2 ± 0.2	−27.1 ± 0.2
			Dimer to Tetramer Assembly Free Energies		
$^0\Delta G_2$	−5.2 ± 1.0	−8.1[b]	−8.4[b]	−9.1[b]	−14.4 ± 0.1
$^4\Delta G_2$	−5.1 ± 1.0	−6.3 ± 0.6	−5.5 ± 0.6	−5.1 ± 0.6	−8.1 ± 0.3
			Intrinsic Tetramer Stepwise Binding Free Energies[c]		
$\Delta G'_{41}$	−7.8 ± 0.2	−7.3 ± 0.2	−6.6 ± 0.2	−6.2 ± 0.2	−5.4 ± 0.1
$\langle \Delta G'_{42,43} \rangle$ [f]	−7.8 ± 0.5	−7.4 ± 0.5	−7.3 ± 0.5	−6.3 ± 0.5	−6.4 ± 0.3
$\Delta G'_{44}$	−7.9 ± 0.2	−7.7 ± 0.2	−7.5 ± 0.3	−8.4 ± 0.3	−8.9 ± 0.5
			Intrinsic Tetramer Stepwise Cooperative Free Energies[d]		
$^1\Delta G'_c$	0.1 ± 0.3	0.6 ± 0.3	1.3 ± 0.3	1.7 ± 0.3	3.0 ± 0.2
$\langle ^{2,3}\Delta G'_c \rangle$	0.1 ± 0.6	0.5 ± 0.6	0.6 ± 0.6	1.6 ± 0.6	2.0 ± 0.3
$^4\Delta G'_c$	0.0 ± 0.3	0.2 ± 0.3	0.4 ± 0.4	−0.5 ± 0.4	−0.6 ± 0.4

[a] Binding curves measured under standard conditions (0.1 M Tris, 0.1 M NaCl, and 1.0 mM Na_2EDTA, pH 7.4 at 21.5 °C) in the presence of the enzyme reduction system of Hayashi et al. (1973). [b] Constrained in the fitting procedure to those values estimated from CO binding kinetic results. [c] Obtained by subtracting subsequent intrinsic stepwise overall binding free energies. [d] From Chu et al. (1984). [e] Also contain the βV1M mutation (see footnote 2). [f] Because of the low populations of doubly and triply oxygenated species, ΔG_{42} and ΔG_{43} could not be determined separately for most mutant species. Values given are half the difference between intrinsic overall binding free energies ΔG_{41} and ΔG_{43}.

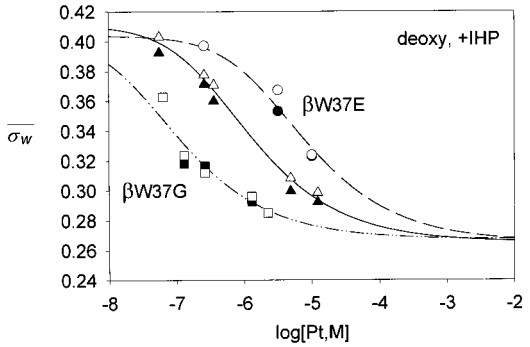

FIGURE 3: Subunit assembly of deoxy-βW37E and deoxy-βW37G in the presence of 500 μM IHP. Weight-average partition coefficients, $\bar{\sigma}_w$ for deoxy-βW37E (circles), deoxy-βW37G (squares), and $CNmetHbA_0$ (triangles) as a function of log [heme] (M). Pairs of data points at each Hb concentration correspond to values determined from the leading (filled symbols) and trailing (open symbols) boundaries of each large-zone experiment. Experimental conditions were 0.1 M Tris, 0.1 M NaCl (0.18 M total chloride), 1 mM EDTA, and 0.5 mM IHP, pH 7.4 at 21.5 °C. 0.01 mM KCN was present during $CNmetHbA_0$ experiments. Smooth curves are dimer to tetramer assembly isotherms simulated using the best fit assembly free energies of −7.25 ± 0.2 kcal/mol (deoxy-βW37E), −8.35 ± 0.2 kcal/mol ($CNmetHbA_0$), and −9.79 ± 0.2 kcal/mol (deoxy-βW37G).

binding isotherms measured in the Gill cell, since at the sample concentration employed (685 mM [heme]) HbA_0 is essentially tetrameric. The value given in Table 3 for $^0\Delta G_2$ of HbA_0 with IHP was measured independently using the haptoglobin kinetics technique (Ip et al., 1976; data not shown).

The large destabilization of the βW37E tetramer results in a population of dimers at 685 mM [heme] that is sufficient to have an appreciable effect on the binding isotherm even in the presence of IHP. Equations 2−4 were therefore used to fit the Gill cell data in order to resolve $^0\Delta G_2$ and the tetramer binding free energies in the presence of IHP, while constraining the overall dimer binding to that of the mutant without IHP. The parameters obtained from this procedure are also given in Table 3. As with HbA_0, IHP reduces overall binding free energy (ΔG_4) and increases stability of the deoxy tetramer. $^0\Delta G_2$ resolved from the fit to the O_2 binding isotherm agreed within error to that measured with AGC. The stepwise binding free energies resolved from the fit are not drastically affected by IHP; binding remains essentially noncooperative with a only very slight increase in affinity at each step.

Effects of Cross-Linking on the O_2 Binding of HbA_0 and βW37E. Both HbA_0 and βW37E were cross-linked between the two αK99 residues. The effects of cross-linking on the binding isotherms of HbA_0 and βW37E are also shown in Figure 4 (unfilled circles and triangles with cross hairs, respectively). Binding parameters resulting from the best fit to a tetramer model for these isotherms are given in Table 3. Isotherms were measured at low total protein concentration in the Imai cell, since presumably the molecules are all tetrameric. Comparison of the α-99 cross-linked HbA_0 binding isotherm with the simulated HbA_0 tetramer isotherm shows that the cross-linked molecule has a slightly decreased affinity for O_2 but maintains essentially the same cooperativity in its stepwise binding. The 1.6 kcal/mol less favorable overall O_2 binding for α-99 cross-linked HbA_0 is due mainly to the final binding step which decreases in affinity from −9.0 kcal/mol of O_2 for HbA_0 to −8.0 kcal/mol for the cross-linked molecule. These results are in agreement with previous O_2 binding studies on this molecule (Vandegriff et al., 1991). Cross-linking βW37E similarly shifts the binding isotherm slightly toward a higher P_{med} and a lower overall binding free energy, but does not substantially change its noncooperative behavior. Affinity at the first binding step is reduced by approximately 0.9 kcal/mol, while affinities of the other binding steps are unchanged.

Effects of IHP on O_2 Binding of Cross-Linked HbA_0 and βW37E. Figure 4 shows the effect of a 50 molar excess of IHP on α-99 cross-linked HbA_0 and βW37E at low concentrations (filled circles and triangles with cross hairs, respectively). Parameters resulting from the fit of a tetramer model to the binding isotherms are listed in Table 3. For clarity, only the curve representing the fit to HbA_0 is shown in Figure 4. The overall binding free energy for cross-linked HbA_0 is reduced by approximately 2.7 kcal/mol upon addition of IHP while the effect is less than 1 kcal/mol for the cross-linked βW37E molecule. While IHP reduces the affinity of

Table 3: Effects of Cross-Linking and IHP on the Thermodynamic Parameters of βW37E and HbA_0 Obtained from Nonlinear Least Squares Fits to Measured O_2 Binding Isotherms[a]

	ΔG_4	ΔG_2	${}^0\Delta G_2$	ΔG_{41}	$\langle\Delta G_{42,43}\rangle$	ΔG_{44}
βW37E						
unmodified	-31.3 ± 0.1	-15.7 ± 0.1	-5.2 ± 0.5	-7.8 ± 0.2	-7.8 ± 0.2	-7.9 ± 0.2
cross-linked[b]	-30.4 ± 0.1			-6.9 ± 0.3	-7.8 ± 0.1	-8.0 ± 0.1
+IHP[c]	-29.7 ± 0.2	-15.7 ± 0.1	-7.3 ± 0.5	-7.2 ± 0.2	-7.4 ± 0.2	-7.6 ± 0.2
cross-linked/+IHP[d]	-29.7 ± 0.2			-6.9 ± 0.2	-7.5 ± 0.2	-7.7 ± 0.2
HbA_0						
unmodified	-27.1 ± 0.1	-16.7 ± 0.1	-14.4 ± 0.1	-5.4 ± 0.1	-6.3 ± 0.1	-9.0 ± 0.1
cross-linked[b]	-25.5 ± 0.2			-5.4 ± 0.1	-6.0 ± 0.1	-8.0 ± 0.1
+IHP[c]	-24.2 ± 0.2		-16.6 ± 0.1[e]	-5.1 ± 0.1	-5.3 ± 1.0	-8.5 ± 1.0
cross-linked/+IHP[d]	-22.8 ± 0.2			-5.1 ± 0.1	-5.3 ± 0.1	-7.1 ± 0.1

[a] Measured under standard conditions (0.1 M Tris, 0.1 M NaCl, and 1.0 mM Na_2EDTA, pH 7.4 at 21.5 °C) with the enzyme reductase system of Hayashi et al. (1973). [b] Cross-linked at the αLys99 positions with a fumaryl group. [c] Approximately 2 mol of IHP/tetramer. [d] 100 mM IHP and 10 mM heme. [e] Measured independently using the haptoglobin kinetics technique (Ip et al., 1976).

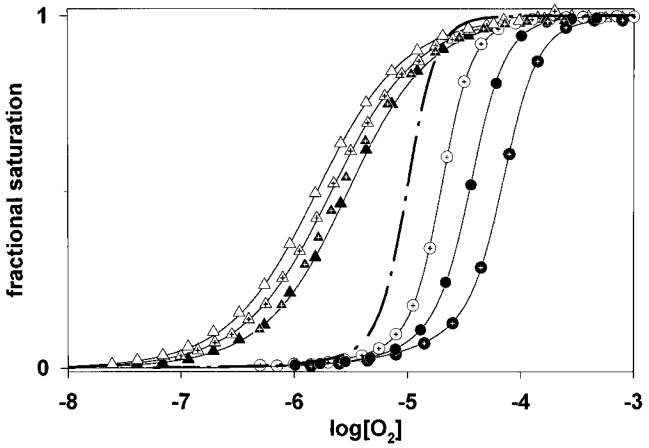

FIGURE 4: Effects of cross-linking and IHP on βW37E and HbA_0 isotherms. Symbols show fractional change in absorbance as a function of log $[O_2]$ measured with the Imai and the Gill cells. Thin solid lines represent least-squares fits using respective stoichiometric models for the various species (see text). Results from the fits are given in Table 3. Experimental conditions were 0.1 M Tris, 0.1 mM NaCl (0.18 mM total chloride), and 1 mM Na_2EDTA, pH 7.4 at 21.5 °C. Curves: (open triangle) βW37E, 635 μM heme; (open triangle with cross-hairs) cross-linked βW37E, 10 μM heme, no IHP; (shaded triangle) βW37E, 685 μM heme, 300 μM IHP; (shaded triangle with cross-hairs) cross-linked βW37E, 10 μM heme, 100 μM IHP; (open circle with cross-hairs) cross-linked HbA_0, 10 μM heme, no IHP; (shaded circle) HbA_0, 610 μM heme, 300 μM IHP; (shaded circle with cross-hairs) cross-linked HbA_0,10 μM heme, 100 μM IHP. The thick dot-dashed line is the theoretical isotherm for a pure solution of HbA_0 tetramers.

$\langle\Delta G'_{42,43}\rangle$ and $\Delta G'_{44}$ for cross-linked HbA_0, it has no appreciable effect on the stepwise binding of cross-linked βW37E.

DISCUSSION

In the present work we describe results and analyses of O_2 binding isotherms measured for a series of recombinant Hbs with mutations at the βW37 position (βW37E, βW37G, βW37A, βW37Y). All mutants in the series were found to show increased affinity and reduced cooperativity compared with normal Hb. The extent of change from wild-type function depends on the particular amino acid substitution; replacing Trp with Tyr, Gly, Ala, and Glu successively shifts the binding isotherms toward lower $[O_2]$ while decreasing their steepness (Figure 1). Probable origins for the increased affinity and decreased cooperativity are (1) increased levels of dissociated $\alpha\beta$ dimers due to tetramer destabilization and/or (2) perturbation of the mutant dimer and tetramer binding properties.

Effects of substitution at the βW37 position on O_2 binding properties has been previously characterized for a number of other recombinant and naturally occurring mutant Hbs. Recombinant Hbs βW37F and βW37T, and the naturally occurring mutant Hbs Howick (βW37G) and Hirose (βW37S) were found, as the mutants of this study, to have increased binding affinity and decreased cooperativity (Brittain, 1994; Fujita, 1972; Ishimori et al., 1992; Owen et al., 1993; Yamaoka, 1971). These effects, however, were attributed mainly to enhanced tetramer to dimer dissociation in which the dimers and tetramers were assumed to bind O_2 with wild-type affinities. Because, in previous studies, measurements were made on dilute samples in which the abundance of tetramers was too low to yield quantitative information on their properties, or because the measurements were made using methods not sufficiently accurate at the very low partial pressures where the binding transitions of these high-affinity mutants occur, such a model was sufficient to account for the observed binding behavior.

In contrast, we have employed the thin-layer method of Gill in which O_2 binding measurements are made at very high Hb concentrations. The high concentrations, through mass action, augment the fraction of tetramer in the sample. In addition, the dilution method of deoxygenation employed by the Gill cell allows detailed isotherm shape information to be obtained at very low O_2 partial pressures—below the accuracy range of electrode methods. Accordingly, it was feasible to resolve for each of the mutants the overall dimer binding free energy and the overall and three of the stepwise tetramer binding free energies. The results establish that mutations at the βW37 position clearly perturb both the dimer to tetramer equilibrium and the binding properties of the dimers and tetramers themselves.

Figure 5 illustrates the failure of fitting the βW37E isotherm assuming (as in previous studies) that the dimer and tetramer binding properties of the mutant Hb are unchanged and that only the dimer association has been unfavorably perturbed from wild type. The best fit of this model to the βW37E isotherm is shown as a dashed line; the residuals from the fit are shown in the upper graph as open circles. For comparison, the solid line (identical with that of Figure 1) represents the fitted curve from our analysis. Fits to the entire series of mutant isotherms that, again,

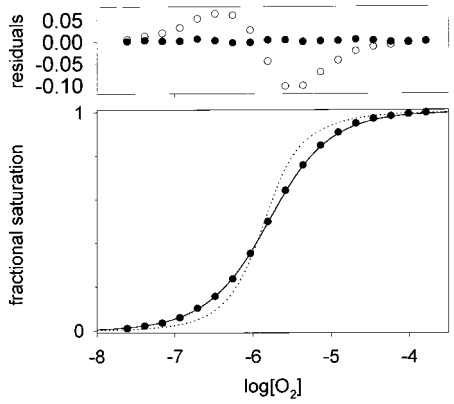

FIGURE 5: Failure of fitting βW37E isotherm assuming only perturbed tetramer assembly. (Lower) Filled circles are the normalized change in absorbance at 415 nm as measured with the Gill cell for the βW37E mutant. The solid line is the curve representing the best fit of the linked dimer and tetramer binding to the data allowing both assembly and stepwise binding constants to vary in the fit. (Data and simulated curve are identical with those of Figure 1.) The dashed line represents the best fit to the βW37E isotherm assuming that mutant dimer and tetramer binding properties are unchanged from wild type and that only the assembly properties are perturbed. (Upper) Residuals from the fit based on our analyses (filled circles) and the fit assuming unchanged tetramer binding free energies (open circles).

assume normal Adair binding constants for the mutant dimers and tetramers and that vary only the association equilibria all yield residuals with a similar unsatisfactory shape and amplitude (data not shown). We can, then, assert with some confidence that the mutant dimer and tetramer binding properties are indeed different from wild type. Our fitting analysis, which allows the dimer and tetramer binding free energy values to vary from wild type, while constraining the deoxy dimer to tetramer assembly free energies to those measured independently gives the results summarized in Table 2.

Of note is that the mutant dimers all show an overall decreased affinity for O_2 of ~1 kcal/mol compared to the wild-type dimers. This alteration of dimer affinity upon Trp substitution is somewhat surprising given that, of 17 previously studied mutant Hbs for which dimer affinities were determined, only one, Hb Kansas (βN102T), showed any major change from wild-type affinity (Turner et al., 1992). Furthermore, the mutation in Hb Kansas, unlike those in this β37 series, is of a residue in direct contact with the heme. In fact, the dimer affinity of the naturally occurring β37 mutant Hb Rothschild has been found to be identical within error to that of wild-type Hb. However, the reduced dimer affinity of the mutant series of this present study is necessary to reconcile the oxygen binding data with independently measured tetramer assembly free energies. Constraining the dimer affinities to that of wild type results in tetramer stabilities much lower than those determined from AGC and kinetic results (data not shown).

Fortunately, determination of the mutant tetramer binding properties is relatively independent of the interplay described above between the $^0\Delta G_2$ and ΔG_2 "arms" of the linkage scheme (see Scheme 1). That is, the tetramer stepwise binding affinities are unchanged whether the overall dimer affinities are constrained to that of wild type or whether the assembly free energies are constrained to the independently measured values. Moreover, it is the pattern of change of the mutant tetramer stepwise free energies from those of a normal cooperative tetramer that is the main interest in our discussion.

Scheme 1

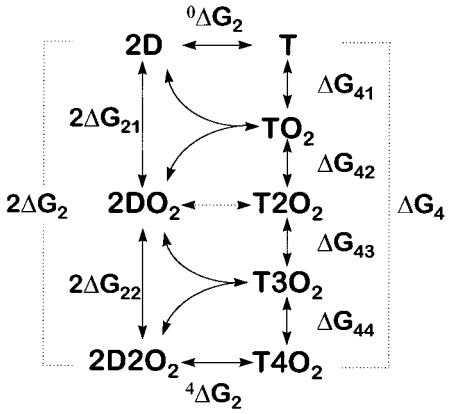

This pattern shows an order in the perturbation from wild-type function and remains unchanged despite the details of analysis. The most disturbed binding behavior is displayed by the βW37E tetramer in that it retains no cooperativity with four stepwise binding free energies that are indistinguishable from that of the dimer. Slight cooperativity may be present in βW37G mutant; the free energy for the last binding step is slightly more favorable that for that of the first. The βW37A mutant then shows a clearly apparent sequential increase in affinity with moles of O_2 bound, and finally, βW37Y has stepwise binding free energies that increase in affinity with a pattern that approaches that of wild-type Hb. The intrinsic stepwise binding free energies for all the mutants and HbA_0 ($\Delta G'_{4n}$, $n = 1-4$)) are given in Table 2.

Also shown in Table 2 are the intrinsic stepwise cooperative free energies ($^n\Delta G_c$, $n = 1-4$) for both the mutant and normal HbA_0 calculated as the difference in the intrinsic stepwise binding free energy for each successive mole of O_2 bound to the tetramer from that of the dimer.[4] Under standard conditions a normal HbA_0 tetramer has an initial O_2 binding step that is 3.0 kcal/mol less favorable than that of the dimer (i.e., $^1\Delta G'_c = 3.0$ kcal/mol). An opposing tertiary structural change by the protein (tertiary constraint) reduces the net affinity of this binding step from that of a dimer; the 3.0 kcal/mol of free energy "penalty" is thus utilized for structural changes that compromise the "T" quaternary form. When a second O_2 binds to a site which is across the $\alpha^1\beta^2$ interface, the T quaternary form is no longer favored and the molecule switches into the "R" structure (i.e., the alternative orientation of dimers). The affinity for O_2 becomes similar to that of dissociated dimers; further ligation-linked structural changes (quaternary enhancement) result in the last O_2 binding step with an affinity 0.8 kcal/mol more favorable than that of the dimer ($^4\Delta G'_c = -0.8$ kcal/mol) (Ackers & Johnson, 1990; Doyle et al., 1992b; Mills & Ackers, 1979).

From the O_2 binding study of the present mutant series we see a progressive decrease in tetramer stability. This decrease in stability reflects a decrease in the tertiary constraint of the initial binding step ($^1\Delta G'_c$)—the more destabilized the tetramer, the higher its affinity at the first binding step. If the tetramer is sufficiently destabilized (as

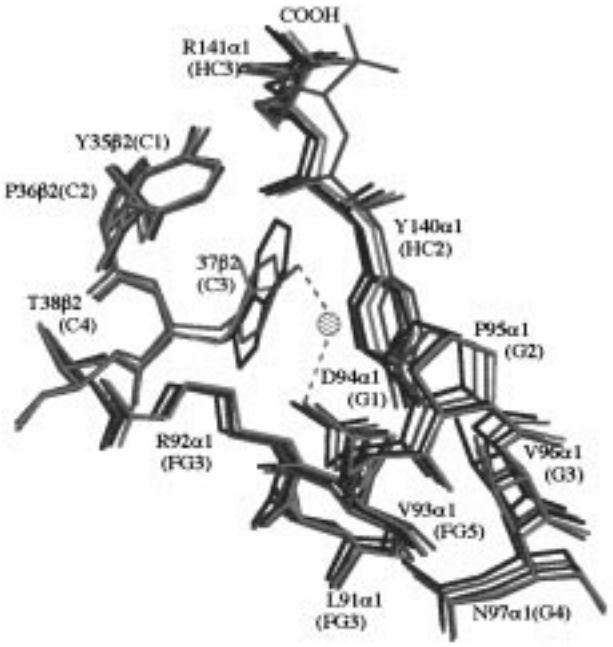

FIGURE 6: Overlay of βV1M and βW37 Hb crystal structures. Atomic models of the deoxy low-salt crystal structures (Kavanaugh et al., 1998) of βV1M (black), βW37Y (green), βW37A (dark blue), βW37G (light blue), and βW37E (red) in the environment of the β37 residue. Models have been overlaid following least-squares "sieve fit" superposition of the β2 subunits. Shown are β2 subunit residues Tyr35β(C1) through Thr38β(C4) and α1 subunit residues Leu91α(FG3) through Asn97α(G4), Tyr140α(HC2), and Arg141α-(HC3). Combined mutation-induced tertiary and quaternary structural changes result in progressive movement of the α1 FG corner and G helix away from the β2 subunit C helix. The approximate magnitudes of the largest combined structural changes (at Pro95α) are 0.0 Å for βV1M, 0.33 Å for βW37Y, 0.57 Å for βW37A, 0.60 Å for βW37G and 0.72 Å for βW37E. [See Kavanaugh et al. (1998) for a complete description.]

in the βW37E and βW37G mutants), we also see apparent loss of the strain which normally builds up in the partially ligated T molecules and eventually triggers the quaternary switch to R; this loss results in completely noncooperative binding.

The high-resolution X-ray crystal structures for the deoxy-βW37 mutant tetramers are in complete support with such an interpretation of the oxygen binding results. The effect on the crystal structure of replacing β37 Trp with any of the residues in the series is always to move the α1 FG corner and G helix *away* from the β2 subunit C helix as illustrated in Figure 6. This movement becomes progressively larger in the same order as seen for the perturbations of free energies of assembly and binding from that of HbA_0: βW37E > βW37G > βW37A > βW37Y. In addition, the temperature factors in the region of the COOH-terminal groups, which are normally among the lowest within the Hb structure, show significant increases as Trp is substituted by Ala, Gly, and finally Glu (Kavanaugh et al., 1998). These observations of the mutant crystal structures indicate that portions of the allosteric core that may provide a steric source for the tertiary strain that accompanies ligation are less tightly packed and more relaxed upon βW37 substitution.

It is not surprising, then, that normal cooperative binding cannot be restored simply by assembling the two mutant dimers together. Cross-linking the molecule at the αK99 position only slightly reduces the affinity of the first binding step (Table 3) but does not affect the two subsequent steps. Such a result not only provides additional strong corroboration that the mutant *tetramer* O_2 binding properties are perturbed from that of normal HbA_0 but also indicates the need for a precise topology in the interface so that cooperative binding may occur. Similarly, IHP, while stabilizing both the βW37E and βW37G mutant tetramers by ~30-fold, only shifts the binding curves slightly toward lower affinity.

Stabilization of the βW37E tetramer by IHP (known to bind preferentially to deoxy-HbA_0), when considered with the barely perturbed T quaternary form of all the mutant crystal structures, indicates that the deoxy mutant tetramers are present in solution in the quaternary T form, despite their high affinity and despite the fact that the molecule appears to have lost most of the structural constraints that impart cooperative binding. The presence of multiple energy levels within the T quaternary structure at equilibrium in solution has be demonstrated for HbA_0 (LiCata et al., 1993) as tertiary constraint and also within the R quaternary structure as quaternary enhancement (Ackers & Johnson, 1990). Although detailed understanding of the structural manifestations of these energetic effects is not yet understood, the characterization of the solution properties of mutant hemoglobin is providing an invaluable tool for demonstrating their presence and importance.

REFERENCES

Ackers, G. K., & Halvorson, H. R. (1974) *Proc. Natl. Acad. Sci. U.S.A. 71*, 4312−4316.

Ackers, G. K., & Smith, F. R. (1985) *Annu. Rev. Biochem. 54*, 597−629.

Ackers, G. K., & Smith, F. R. (1986) *Biophys. J. 49*, 155−165.

Ackers, G. K., & Johnson, M. L. (1990) *Biophys. Chem. 37*, 265−279.

Baldwin, J., & Chothia, C. (1979) *J. Mol. Biol. 129*, 175−220.

Brittain, T. (1994) *Biochem. J. 300*, 553−556.

Chatterjee, R., Welty, E. V., Walder, R. Y., Pruitt, S. L., Rogers, P. H., Arnone, A., & Walder, J. A. (1986) *J. Biol. Chem. 261*, 9929−9937.

Chu, A. H., Turner, B. W., & Ackers, G. K. (1984) *Biochemistry 23*, 604−617.

DiCera, E., & Gill, S. J. (1988) *Biophys. Chem. 29*, 351−356.

Dickerson, R. E., & Geis, I. (1983) *Hemoglobin: structure, function, evolution, and pathology*, Benjamin/Cummings, Menlo Park, CA.

Dolman, D., & Gill, S. J. (1978) *Anal. Biochem. 87*, 127−134.

Doyle, M. L., & Ackers, G. K. (1992) *Biochemistry 31*, 11182−11195.

Doyle, M. L., Lew, G., De Young, A., Kwiatkowski, L., Wierzba, A., Noble, R. W., & Ackers, G. K. (1992a) *Biochemistry 31*, 8629−8639.

Doyle, M. L., Lew, G., Turner, G. J., Rucknagel, D., & Ackers, G. K. (1992b) *Proteins 14*, 351−362.

Fujita, S. (1972) *J. Clin. Invest. 51*, 2520−2529.

Hayashi, A., Suzuki, T., & Shin, M. (1973) *Biochim. Biophys. Acta 310*, 309−316.

Hernan, R. A., Hui, H. L., Andracki, M. E., Noble, R. W., Sligar, S. G., Walder, J. A., & Walder, R. Y. (1992) *Biochemistry 31*, 8619−8628.

Huang, Y., & Ackers, G. K. (1995) *Biochemistry 34*, 6316−6327.

Imai, K. (1981) *Methods Enzymol. 76*, 438−449.

Ip, S. H., Johnson, M. L., & Ackers, G. K. (1976) *Biochemistry 15*, 654−660.

Ishimori, K., Imai, K., Miyazaki, G., Kitagawa, T., Wada, Y., Morimoto, H., & Morishima, I. (1992) *Biochemistry 31*, 3256−3264.

Johnson, M. L., & Frasier, S. G. (1985) *Methods Enzymol. 117*, 308−313.
Johnson, M. L., Halvorson, H. R., & Ackers, G. K. (1976) *Biochemistry 15*, 5363−5371.
Kwiatkowski, L. D., Hui, H. L., Wierzba, A., Noble, R. W., Walder, R. Y., Peterson, E. S., Sligar, S. G., & Sanders, K. E. (1998) *Biochemistry 37*, 4325−4335.
LiCata, V. J., Dalessio, P. M., & Ackers, G. K. (1993) *Proteins 17*, 279−296.
Mills, F. C., & Ackers, G. K. (1979) *Proc. Natl. Acad. Sci. U.S.A. 76*, 273−277.
Mills, F. C., Johnson, M. L., & Ackers, G. K. (1976) *Biochemistry 15*, 5350−5362.
Mills, F. C., Ackers, G. K., Gaud, H. T., & Gill, S. J. (1979) *J. Biol. Chem. 254*, 2875−2880.
Owen, M. C., Ockelford, P. A., & Wells, R. M. (1993) *Hemoglobin 17*, 513-521.
Perutz, M. F. (1970) *Nature 228*, 726−739.
Peterson, E. S., & Friedman, J. M. (1998) *Biochemistry 37*, 4346−4357.
Robert, C. H., Fall, L., & Gill, S. J. (1988) *Biochemistry 27*, 6835−6843.
Sasaki, J., Imamura, T., & Yanase, T. (1978) *J. Biol. Chem. 253*, 87−94.
Sharma, V. S., Newton, G. L., Ranney, H. M., Ahmed, F., Harris, J. W., & Danish, E. H. (1980) *J. Mol. Biol. 144*, 267−280.
Turner, G. J., Galacteros, F., Doyle, M. L., Hedlund, B., Pettigrew, D. W., Turner, B. W., Smith, F. R., Moo-Penn, W., Rucknagel, D. L., & Ackers, G. K. (1992) *Proteins 14*, 333−350.
Valdes, R., Jr., & Ackers, G. K. (1979) *Methods Enzymol. 61*, 125−142.
Vallone, B., Bellelli, A., Miele, A. E., Brunori, M., & Fermi, G. (1996) *J. Biol. Chem. 271*, 12472−12480.
Vandegriff, K. D., Le Tellier, Y. C., Winslow, R. M., Rohlfs, R. J., & Olson, J. S. (1991) *J. Biol. Chem. 266*, 17049−17059.
White, S. L. (1976) *J. Biol. Chem. 251*, 4763−4769.
Wilhelm, E., Battino, R., & Wilcock, R. J. (1977) *Chem. Rev. 77*, 219−262.
Williams, R. C., Jr., & Tsay, K. Y. (1973) *Anal. Biochem. 54*, 137−145.
Yamaoka, K. (1971) *Blood 38*, 730−738.

BI970868A